IJE TRANSACTIONS C: Aspects Vol. 27, No. 3, (March 2014) 475-486

International Journal of Engineering

Journal Homepage: www.ije.ir

# Analytical Solutions of Stress Field in Adhesively Bonded Composite Single-lap Joints under Mechanical Loadings

E. Selahi, M. Tahani*, S. A. Yousefsani

*Department of Mechanical Engineering, Faculty of Engineering, Ferdowsi University of Mashhad, Mashhad, Iran*

*PAPER INFO*

*Paper history:*
Received 27 February 2013
Received in revised form 29 June 2013
Accepted 22 August 2013

*Keywords*:
Adhesive Bonding
Composite Joint
Interlaminar Stress
Analytical Solution

*ABSTRACT*

In this paper, considering an adhesively bonded composite single-lap joint, a novel approach is presented to predict the peel and shear stress distributions of the adhesive layer for an ASTM standard test sample. In the current method, the equilibrium equations are derived using the energy method and based on the Timoshenko's beam theory. Two solution procedures then are discussed; one of them represents a solution approach based on the direct variational method allied with use of the Ritz approximation; while the second one is based on a linear estimating function. Unlike previous methods, in which the variation of stress through the thickness of adhesive is neglected or is assumed to be linear and they cannot be used to analyze the joints with thick adhesive layers; considering the effects of adhesive thickness makes it possible to employ present method to analyze the joints with thick adhesive layers as well as thin ones.

**doi:** *10.5829/idosi.ije.2014.27.03c.16*

## 1. INTRODUCTION

Recently, use of fiber reinforced composites has been widely increased due to their special improved properties such as low weight, high relative strength ($\sigma_u/\rho$) and relative stiffness ($E/\rho$), and also good corrosion resistance (e.g. in glass fibers). As an instance, most of panels and shells used for construction of light planes in the aviation industries are made of fiber reinforced composites, and the adhesively bonded joints are used for joining them to the stiffeners, wing spars, and frames, which can also be made of composite materials [1, 2].

Nowadays, use of mechanical joints such as pivots and bolts in composite structures has decreased because high stress concentrations exists near the holes, their adding weights, and also weak resistance to corrosion around the joining regions. Adhesive bonding is the most prevalent and appropriate joining method in construction of composite structures.

Adhesive bonding is a joining process which is widely used to connect at least two species in particularly composite structures to do some tasks they cannot perform, solitarily. Nowadays, adhesively bonded joints are widely used in composite structures. Because of the large and mostly continuous joining surface on which the forces are distributed, the adhesive joints have lower stress concentration in comparison with mechanical ones. Moreover, their low costs, higher relative stiffness, better sealing capabilities, and some other advantages make them more efficient and operative to use.

One of the most important aspects of the analysis of adhesively bonded joints is to determine how the stresses are distributed along the bonding region and through the thickness of the adhesive layer and particularly around the free edges of the bonding region in which the failure may start.

Most of presented analytical methods assume the adhesive layer to be very thin, and so, variations of stresses through the thickness of the adhesive are ignored; while, experimental investigations have clearly shown that the load carrying capacity of the adhesive joints decreases by increasing the adhesive thickness [2-4]. Therefore, designing the joint with this assumption may result in destruction and failure of joints with thick adhesive layers.

The first efforts about the analysis of adhesive joints were made by Volkersen [5] in 1938. He studied an

*Corresponding Author Email: mtahani@um.ac.ir (M. Tahani)

adhesively bonded single-lap joint (SLJ) in which the adhesive layer was modeled as continuous shear springs. In his model, the effects of bending moment caused due to eccentricity of loading axes were ignored. Afterwards, Goland and Reissner [6] modified the Volkersen's theory by introducing the adhesive layer as continuous shear and normal springs.

Most researches on the analysis of adhesive joints have been performed in 1973 by Hart-Smith [7-9] who presented some methods to investigate the single- and double-lap, stepped, and scarf adhesive joints with isotropic materials in which the adhesive layer is modeled as a linear elastic material. Adams and Peppiat [10] demonstrated that there is lateral shear stress through the thickness of the adhesive layer, which is often neglected because of its smaller value in comparison with longitudinal shear stress.

Bogdanovich and Kizhakkethara [11] simulated an adhesively bonded composite double-lap joint (DLJ) using three-dimensional finite element method. Rao and coworkers [12, 13] provided static analyses of adhesively bonded composite/hybrid single-lap joints using the finite element method based on the three-dimensional theory of elasticity, and determined the transverse peel and shear stresses at the bonding lines and mid-surface of the adhesive. They found out that three-dimensional stress analysis approach is needed to analyze the composite joints.

Considering the relatively thin adhesive layer as simple tensile-compressive elastic springs, Krishna et al. [14] modeled an adhesively bonded composite single-lap joint using the finite element method. Selahi et al. [15-20] investigated some common and uncommon adhesively bonded composite joints, and studied the influences of geometrical dimensions and the spew fillets at boundaries of the joint.

Based on the Timoshenko's beam theory for the transverse shear deformations, Chen and Qiao [21] presented a theoretical model of adhesive joints using the first-order shear deformation theory. They assumed the longitudinal normal stress varies linearly through the adhesive thickness, and determined the stresses at the bonding lines (interfacial stresses) as well as through thickness of adhesive layer.

Diaz et al. [22] employed an analytical layered (semi-layerwise) approach to model the classical double-lap joints. Their model, in contrast with several present methods, assumes the linear variation of transverse stresses through each physical layer, and in this manner, their model represents more accurate results compared with other simple theories.

Yousefsani and Tahani [23, 24] presented analytical solutions to interlaminar stresses through the adhesive thickness and along the bond-lines of adhesively bonded single- and double-lap composite joints using the full layerwise theory, and studied the edge effects on the peel, shear, and von Mises stress distributions. They also investigated the effects of adhesive thickness, different static loadings, and inhomogeneity of materials.

Da Silva et al. [25, 26] reported a review on several analytical methods for analysis of single- and double-lap joints. They compared available methods as well as their advantages and limitations from several standpoints, such as the linearity/non-linearity of material properties and the analysis approach, two- or three-dimensionality of models, solution accuracy, solution time, material elasticity/plasticity, etc.

They found that most of present methods provide two-dimensional stress analysis approaches assuming plane stress or plane strain states. Moreover, the non-linear material properties are not considered in most of present methods due to complexity of solution procedure.

In this paper, a new analytical method to stress analysis of adhesively bonded composite SLJs with fixed-free and pin-roll end conditions subjected to axial tensile load and bending moment are presented. The equilibrium equations are obtained using energy method based on Timoshenko's beam theory and including the effects of adhesive thickness. The previous methods, in which the variation of interfacial stresses through the thickness of adhesive layer is neglected or is assumed to be linear, cannot accurately analyze the joints with thick adhesive layers. The present method can be easily employed to analyze these joints as well as joint with thin adhesive layers.

## 2. MATHEMATICAL MODELING

Each adhesive joint consists of two regions (i.e., the overlap region and outside of it) with different governing equations. It should be noted that, for the inside of overlap, where the joining is performed, the governing equations are more complex than those outside of it. In this research, adhesively bonded SLJ as shown in Figure 1 is chosen for study in order to reduce the number of governing equations. However, the relations presented here can be easily extended to other kinds of adhesive joints.

### 2. 1. Modeling of the Overlap Region

**2. 1. 1. Adherends** Using Taylor's series, each displacement component can be expanded as infinite sum of terms that are calculated from the values of that component's derivatives at mid-plane of the plate. In the first-order shear deformation plate theory, the displacement components are assumed as:

$$\begin{aligned} u(x, y, z) &= u_0(x, y) + z\psi_x(x, y) \\ v(x, y, z) &= v_0(x, y) + z\psi_y(x, y) \\ w(x, y, z) &= w_0(x, y) + z\psi_z(x, y) \end{aligned} \quad (1)$$

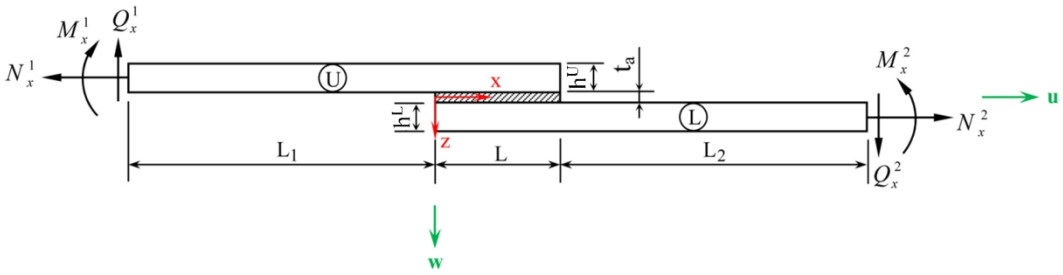


**Figure 1.** Schematic view of a common adhesively bonded SLJ.

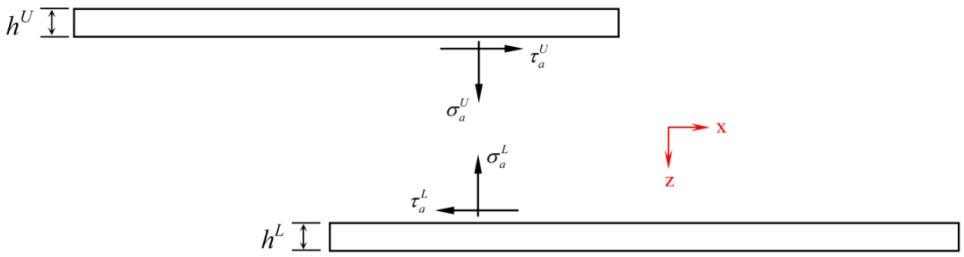


**Figure 2.** Schematic view of the upper and lower adherends.

In Equation (1), the functions $\psi_x$ and $\psi_y$ are the rotation functions, $\psi_z(x,y)$ denotes thickness change of the plate, and $z$ denotes the thickness coordinate. Also, $u_0(x,y)$, $v_0(x,y)$, and $w_0(x,y)$ represent the displacement components of the points on the middle surface of the plate in the $x$-, $y$-, and $z$-directions, respectively.

Moreover, $u(x,y,z)$, $v(x,y,z)$, and $w(x,y,z)$ indicate the displacement components of any material point in the region in the $x$-, $y$-, and $z$-directions, respectively.

Here, the adherends are assumed to be made of orthotropic laminae with symmetric or asymmetric stacking sequences. Moreover, since the joint width is assumed to be small, the displacement field introduced in Equation (1) can be safely simplified based on Timoshenko's beam theory. By modeling the adherends as beams, it is almost safe to ignore the lateral displacement $v(x,y,z)$. Furthermore, it is assumed that $\varepsilon_z = 0$, which means $w(x,y,z) = w_0(x,y)$. Therefore, the assumed displacements can be expressed as follows:

$$\begin{aligned} u &= u_0(x) + z\psi(x) \\ w &= w_0(x) \end{aligned} \tag{2}$$

Using Equation (1), the force and moment resultants can be represented as follows:

$$\begin{aligned} N_x &= A_{11}\frac{du_0(x)}{dx} + B_{11}\frac{d\psi(x)}{dx} \\ M_y &= B_{11}\frac{du_0(x)}{dx} + D_{11}\frac{d\psi(x)}{dx} \\ Q_z &= k_s A_{55}\left(\psi_x(x) + \frac{dw(x)}{dx}\right) \end{aligned} \tag{3}$$

where $A_{ij}$, $B_{ij}$, and $D_{ij}$ represent the extensional, coupling, and bending stiffnesses, respectively, as:

$$\begin{aligned} A_{ij} &= \sum_{k=1}^{n} \bar{Q}_{ij}^{(k)}(z_k - z_{k-1}) \\ B_{ij} &= \frac{1}{2}\sum_{k=1}^{n} \bar{Q}_{ij}^{(k)}(z_k^2 - z_{k-1}^2) \\ D_{ij} &= \frac{1}{3}\sum_{k=1}^{n} \bar{Q}_{ij}^{(k)}(z_k^3 - z_{k-1}^3) \end{aligned} \tag{4}$$

In Equation (3), $k_s$ is the shear correction factor introduced in the first-order shear deformation theories. Equation (3) can be solved to obtain derivatives of displacement components as:

$$\begin{aligned} u_{0,x} &= \frac{D_{11}N_x - B_{11}M_y}{A_{11}D_{11} - B_{11}^2} \\ \psi_{,x} &= \frac{B_{11}N_x - A_{11}M_y}{B_{11}^2 - A_{11}D_{11}} \\ w_{,x} &= \frac{1}{k_s A_{55}}Q_z - \psi_x \end{aligned} \tag{5}$$

Figure 2 illustrates both upper and lower adherends in the bonding region. In this figure, the subscript index $a$ and superscript indices $U$ and $L$ are used to indicate the adhesive layer, and the upper and lower adherends, respectively (e.g., $\tau_a^U$ in Figure 2 represents the shear stress on the upper boundary of adhesive layer). Upon substitution of Equation (2) into the linear strain-displacement relations of elasticity, the following nonzero strain components will be obtained:

$$\varepsilon_{xx}=\frac{\partial u}{\partial x}=\frac{du_{\circ}}{dx}+z\frac{d\psi_x}{dx}$$
$$\gamma_{xz}=\frac{\partial u}{\partial z}+\frac{\partial w}{\partial x}=\psi_x+\frac{dw}{dx} \quad (6)$$

Thus, the statement of variation of strain energy for the adherends may be expressed as follows:

$$\begin{aligned}\delta U&=\int_V \sigma_{ij}\delta\varepsilon_{ij}dV\\&=\int_0^L\iint_A\left(\sigma_{xx}\delta\gamma_{xx}+\tau_{xz}\delta\gamma_{xz}\right)dAdx\\&=\int_0^L\iint_A\left\{\sigma_{xx}\left(\frac{d\delta u_{\circ}}{dx}+z\frac{d\delta\psi_x}{dx}\right)+\tau_{xz}\left(\delta\psi_x+\frac{d\delta w}{dx}\right)\right\}dAdx\\&=\int_0^L\left\{N_x\frac{d\delta u_{\circ}}{dx}+M_y\frac{d\delta\psi_x}{dx}+Q_z\left(\delta\psi_x+\frac{d\delta w}{dx}\right)\right\}dx\\&=\int_0^L\left\{-\frac{dN_x}{dx}\delta u_{\circ}-\frac{dM_y}{dx}\delta\psi_x+Q_z\delta\psi_x\right.\\&\left.-\frac{dQ_z}{dx}\delta w\right\}dx+\left[N_x\delta u_{\circ}+M_y\delta\psi_x+Q_z\delta w\right]_0^L\end{aligned} \quad (7)$$

where $L$ is the length of the overlap. On the other hand, the expressions of virtual works done on the upper and lower adherends by external forces are written as below:

$$\delta V^U=\int_0^L\left(\tau_a{}^U\delta u_{\circ}^U+\sigma_a{}^U\delta w^U+\frac{h^U}{2}\tau_a{}^U\delta\psi_x^U\right)dx$$
$$\delta V^L=\int_0^L\left(\tau_a{}^L\delta u_{\circ}^L+\sigma_a{}^L\delta w^L-\frac{h^L}{2}\tau_a{}^L\delta\psi_x^L\right)dx \quad (8)$$

The summations of $\delta U$ and $\delta V$ represent the total potential energy which does not change in static equilibrium condition (i.e., $\delta(U+V)=0$). Therefore, the equilibrium equations of the upper and lower adherends are obtained as:

$$\delta u_{\circ}^U:\frac{dN_x^U}{dx}=-\tau_a^U,\quad \delta w^U:\frac{dQ_z^U}{dx}=-\sigma_a^U$$
$$\delta\psi_x^U:\frac{dM_y^U}{dx}=Q_z^U-\frac{h^U}{2}\tau_a^U$$
$$\delta u_{\circ}^L:\frac{dN_x^L}{dx}=\tau_a^L,\quad \delta w^L:\frac{dQ_z^L}{dx}=\sigma_a^L$$
$$\delta\psi_x^L:\frac{dM_y^L}{dx}=Q_z^L-\frac{h^L}{2}\tau_a^L \quad (9)$$

**2. 1. 2. Adhesive layer** In this paper, it is assumed that the normal stress along the $x$-direction in the isotropic adhesive layer can be neglected. Hence, there are only the peel and shear stresses, $\sigma_{a,z}$ and $\tau_{a,xz}$, existing in the adhesive layer. With the assumption of the plane-strain condition, the relation between the strains $\varepsilon_{a,x}$ and $\varepsilon_{a,z}$ is:

$$\varepsilon_{a,x}=-\frac{\nu}{1-\nu}\varepsilon_{a,z} \quad (10)$$

By indicating the displacement components of the adhesive layer in the $x$- and $z$-directions as $u_a(x,z)$ and $w_a(x,z)$, respectively, the peel and shear stresses can be written as below:

$$\begin{aligned}\sigma_{a,z}&=\frac{E}{(1+\nu)(1-2\nu)}\left[\nu\varepsilon_{a,x}+(1-\nu)\varepsilon_{a,z}\right]\\&=\frac{E}{1-\nu^2}\varepsilon_{a.z}=\frac{E}{1-\nu^2}\frac{\partial w_a}{\partial z}\\\tau_{a,xz}&=G\left(\frac{\partial u_a}{\partial z}+\frac{\partial w_a}{\partial x}\right)\end{aligned} \quad (11)$$

where $E$, $G$, and $\nu$ represent Young's modulus, shear modulus, and Poisson's ratio of the adhesive, respectively. Moreover, the adhesive thickness is set to be $t_a$. As previously discussed, interfacial peel and shear stresses of the adhesive layer are introduced as:

$$\tau_a{}^U=-\tau_{a,xz}\Big|_{Z=-\frac{t_a}{2}},\quad \tau_a{}^L=-\tau_{a,xz}\Big|_{Z=\frac{t_a}{2}}$$
$$\sigma_a{}^U=-\sigma_{a,z}\Big|_{Z=-\frac{t_a}{2}},\quad \sigma_a{}^L=-\sigma_{a,z}\Big|_{Z=\frac{t_a}{2}} \quad (12)$$

The variation of the strain energy of the adhesive layer may be written as follows:

$$\begin{aligned}\delta U&=\int_V\sigma_{ij}\delta\varepsilon_{ij}dV\\&=\int_0^L\int_A\left(\sigma_{a,z}\delta\varepsilon_{a,z}+\tau_{a,xz}\delta\gamma_{a,xz}\right)dAdx\\&=\int_0^L\int_A\left[\frac{E}{1-\nu^2}\frac{\partial w_a}{\partial z}\frac{\partial\delta w_a}{\partial z}+G\left(\frac{\partial w_a}{\partial x}+\frac{\partial u_a}{\partial z}\right)\right.\\&\left.\left(\frac{\partial\delta w_a}{\partial x}+\frac{\partial\delta u_a}{\partial z}\right)\right]dAdx\\&=\int_0^L\int_{\frac{-t_a}{2}}^{\frac{t_a}{2}}\left[\frac{-E}{1-\nu^2}\frac{\partial^2 w_a}{\partial z^2}\delta w_a-G\left(\frac{\partial^2 w_a}{\partial x^2}\delta w_a\right.\right.\\&\left.\left.+\frac{\partial^2 w_a}{\partial x\partial z}\delta u_a+\frac{\partial^2 u_a}{\partial x\partial z}\delta w_a+\frac{\partial^2 u_a}{\partial z^2}\delta u_a\right)\right]dzdx\\&+\int_0^L\left[\frac{E}{1-\nu^2}\frac{\partial w_a}{\partial z}\delta w_a+\frac{\partial w_a}{\partial x}\delta u_a\right.\\&\left.+\frac{\partial u_a}{\partial z}\delta u_a\right]_{\frac{-t_a}{2}}^{\frac{t_a}{2}}dx+\int_{\frac{-t_a}{2}}^{\frac{t_a}{2}}\left[\frac{\partial w_a}{\partial x}\delta w_a+\frac{\partial u_a}{\partial z}\delta w_a\right]_o^L dz\end{aligned} \quad (13)$$

Next, using the principle of minimum total potential energy, the equilibrium equations are obtained as:

$$\delta u_a : \ \frac{\partial^2 w_a}{\partial x \partial z} + \frac{\partial^2 u_a}{\partial z^2} = 0 \tag{14}$$

$$\delta w_a : \ \frac{E}{1-\nu^2}\frac{\partial^2 w_a}{\partial z^2} + G\frac{\partial^2 w_a}{\partial x^2} + G\frac{\partial^2 u_a}{\partial z \partial x} = 0 \tag{15}$$

In what follows, two methods will be suggested and discussed to define $u_a(x,z)$ and $w_a(x,z)$.

**2. 1. 3. First Method** Here, the direct variational method is employed to obtain solutions for $u_a(x,z)$ and $w_a(x,z)$. Multiplying Equations (14) and (15) by the weight functions $v_1(z)$ and $v_2(z)$, respectively, and integrating the subsequent results yield:

$$\begin{aligned} 0 &= \int_{\frac{-t_a}{2}}^{\frac{t_a}{2}} v_1 \left[ \frac{E}{1-\nu^2}\frac{\partial^2 w_a}{\partial z^2} + G\frac{\partial^2 w_a}{\partial x^2} + G\frac{\partial^2 u_a}{\partial z \partial x} \right] dz \\ &= \int_{\frac{-t_a}{2}}^{\frac{t_a}{2}} \left[ \frac{-E}{1-\nu^2}\frac{\partial w_a}{\partial z}\frac{\partial v_1}{\partial z} + G v_1 \frac{\partial^2 w_a}{\partial x^2} - G\frac{\partial v_1}{\partial z}\frac{\partial u_a}{\partial x} \right] dz \\ &\quad + \left[ \frac{v_1 E}{1-\nu^2}\frac{\partial w_a}{\partial z} + G v_1 \frac{\partial u_a}{\partial x} \right]_{\frac{-t_a}{2}}^{\frac{t_a}{2}} \end{aligned} \tag{16}$$

$$\begin{aligned} 0 &= \int_{\frac{-t_a}{2}}^{\frac{t_a}{2}} v_2 \left[ \frac{\partial^2 w_a}{\partial x \partial z} + \frac{\partial^2 u_a}{\partial z^2} \right] dz \\ &= \int_{\frac{-t_a}{2}}^{\frac{t_a}{2}} \left[ -\frac{\partial v_2}{\partial z}\frac{\partial w_a}{\partial x} - \frac{\partial v_2}{\partial z}\frac{\partial u_a}{\partial z} \right] dz \quad + \left[ v_2 \frac{\partial w_a}{\partial x} + v_2 \frac{\partial u_a}{\partial z} \right]_{\frac{-t_a}{2}}^{\frac{t_a}{2}} \end{aligned} \tag{17}$$

Next, the Ritz approximate method is used to define $w_a$ and $u_a$ as follows:

$$w_a(x,z) = \sum_{j=1}^{M} f_j(x)\phi_j(z), \quad u_a(x,z) = \sum_{j=1}^{N} g_j(x)\psi_j(z) \tag{18}$$

where $\phi_j(z)$ and $\psi_j(z)$ are, respectively, the weight functions $v_1(z)$ and $v_2(z)$ defined in Equations (16) and (17). It is to be noted that these weighting functions must satisfy the essential boundary conditions. Therefore, Equations (16) and (17) will be rewritten as:

$$\begin{aligned} &\int_{\frac{-t_a}{2}}^{\frac{t_a}{2}} \left[ \frac{-E}{1-\nu^2}\frac{\partial \varphi_i}{\partial z}\sum_{j=1}^{M} f_j \frac{\partial \varphi_j}{\partial z} + G\varphi_i \sum_{j=1}^{M}\frac{\partial^2 f_j}{\partial x^2}\varphi_j - G\frac{\partial \varphi_i}{\partial z}\sum_{j=1}^{N}\frac{\partial g_j}{\partial x}\psi_j \right] dz \\ &+ \left[ \frac{E}{1-\nu^2}\varphi_i \sum_{j=1}^{M} f_j \frac{\partial \varphi_j}{\partial z} + G\varphi_i \sum_{j=1}^{N}\frac{\partial g_j}{\partial x}\psi_j \right]_{\frac{-t_a}{2}}^{\frac{t_a}{2}} = 0 \end{aligned} \tag{19}$$

$$\begin{aligned} &\int_{\frac{-t_a}{2}}^{\frac{t_a}{2}} \left[ -\frac{\partial \psi_i}{\partial z}\sum_{j=1}^{M}\frac{\partial f_j}{\partial x}\varphi_j - \frac{\partial \psi_i}{\partial z}\sum_{j=1}^{N} g_j \frac{\partial \psi_j}{\partial z} \right] dz \\ &+ \left[ \psi_i \sum_{j=1}^{M}\frac{\partial f_j}{\partial x}\varphi_j + \psi_i \sum_{j=1}^{N} g_j \frac{\partial \psi_j}{\partial z} \right]_{\frac{-t_a}{2}}^{\frac{t_a}{2}} = 0 \end{aligned} \tag{20}$$

The matrix form of the equations above is:

$$\begin{aligned} &\begin{bmatrix} [A] & [0] \\ [0] & [0] \end{bmatrix} \begin{bmatrix} \{f''\} \\ \{g''\} \end{bmatrix} + \begin{bmatrix} [0] & [B] \\ [C] & [0] \end{bmatrix} \begin{bmatrix} \{f'\} \\ \{g'\} \end{bmatrix} \\ &+ \begin{bmatrix} [D] & [0] \\ [0] & [E] \end{bmatrix} \begin{bmatrix} \{f\} \\ \{g\} \end{bmatrix} = \begin{bmatrix} \{0\} \\ \{0\} \end{bmatrix} \end{aligned} \tag{21}$$

where

$$\begin{aligned} A_{ij} &= G\int_{\frac{-t_a}{2}}^{\frac{t_a}{2}} \varphi_I \varphi_j dz \\ B_{ij} &= G\int_{\frac{-t_a}{2}}^{\frac{t_a}{2}} \frac{-\partial \varphi_i}{\partial z}\psi_j dz + G\left[\varphi_I \psi_j\right]_{\frac{-t_a}{2}}^{\frac{t_a}{2}} \\ C_{ij} &= \int_{\frac{-t_a}{2}}^{\frac{t_a}{2}} \frac{-\partial \psi_i}{\partial z}\varphi_j dz + \left[\psi_I \varphi_j\right]_{\frac{-t_a}{2}}^{\frac{t_a}{2}} \\ D_{ij} &= \int_{\frac{-t_a}{2}}^{\frac{t_a}{2}} \frac{-E}{1-\nu^2}\frac{\partial \varphi_i}{\partial z}\frac{\partial \varphi_j}{\partial z} dz + \left[ \frac{E}{1-\nu^2}\varphi_i \frac{\partial \varphi_j}{\partial z} \right]_{\frac{-t_a}{2}}^{\frac{t_a}{2}} \\ E_{ij} &= \int_{\frac{-t_a}{2}}^{\frac{t_a}{2}} \frac{-\partial \psi_i}{\partial z}\frac{\partial \psi_j}{\partial z} dz + \left[ \psi_i \frac{\partial \psi_j}{\partial z} \right]_{\frac{-t_a}{2}}^{\frac{t_a}{2}} \end{aligned} \tag{22}$$

Next, assuming $[S_1]$ and $[S_2]$ as the matrices of roots of Equation (21), the answers for $f(x)$ and $g(x)$ can be obtained as follows:

$$\begin{bmatrix} \{f(x)\} \\ \{g(x)\} \end{bmatrix} = k_1 e^{[S_1]x} + k_2 e^{[S_2]x} \tag{23}$$

Now, by denoting the functions $f_j(x)$ and $g_j(x)$ for $j = 1, 2, \ldots, M$, the appropriate functions $w_a(x,z) = \sum_{j=1}^{M} f_j(x)\varphi_j(z)$ and $u_a(x,z) = \sum_{j=1}^{N} g_j(x)\psi_j(z)$ may be estimated, easily. Then, the peel and shear stresses $\sigma_{a,z}$ and $\tau_{a,xz}$ can be defined using Equation (11) at each point of the adhesive layer (including $\sigma_a^L$, $\sigma_a^U$, $\tau_a^L$, and $\tau_a^U$). Now, the previously discussed parameters for the adherends may be written as follows:

$$
\begin{aligned}
&Q_z^U = -\int_x \sigma_a^U dx + C_1, \quad Q_z^L = \int_x \sigma_a^L dx + C_7\\
&N_x^U = -\int_x \tau_a^U dx + C_2, \quad N_x^L = \int_x \tau_a^L dx + C_8\\
&M_y^U = \int_x \left( Q_z^U - \frac{h^U}{2}\tau_a^U \right) dx + C_3\\
&M_y^L = \int_x \left( Q_z^L - \frac{h^L}{2}\tau_a^L \right) dx + C_9\\
&u_0^U = \int_x \frac{D_{11}^U N_x^U - B_{11}^U M_y^U}{A_{11}^U D_{11}^U - B^{U2}_{11}} dx + C_4\\
&u_0^L = \int_x \frac{D_{11}^L N_x^L - B_{11}^L M_y^L}{A_{11}^L D_{11}^L - B^{L2}_{11}} dx + C_{10}\\
&\psi_x^U = \int_x \frac{B_{11}^U N_x^U - A_{11}^U M_y^U}{B^{U2}_{11} - A_{11}^U D_{11}^U} dx + C_5\\
&\psi_x^L = \int_x \frac{B_{11}^L N_x^L - A_{11}^L M_y^L}{B^{L2}_{11} - A_{11}^L D_{11}^L} dx + C_{11}\\
&w^U = \int_x \left( \frac{1}{k_s A_{55}^U} Q_z^U - \psi_x^U \right) dx + C_6,\\
&w^L = \int_x \left( \frac{1}{k_s A_{55}^L} Q_z^L - \psi_x^L \right) dx + C_{12}
\end{aligned}
\tag{24}
$$

where the coefficients $C_1$ to $C_{12}$ may be obtained from the boundary conditions at the start or the end points of the inside of the overlap region. These boundary conditions include determination of $u_\circ^U$, $\psi_x^U$, $w^U$, $N_x^U$, $Q_z^U$, $M_y^U$, $N_x^L$, $Q_z^L$, and $M_y^L$ at $x$=0 and $N_x^U$, $Q_z^U$, and $M_y^U$ at $x$=$L$ (see Figure 1). It is to be noted that, $N_x^L$, $Q_z^L$, and $M_y^L$ at $x$=0 and $N_x^U$, $Q_z^U$, and $M_y^U$ at $x$=$L$ must satisfy the free-end conditions; while, $u_\circ^U$, $\psi_x^U$, $w^U$, $N_x^U$, $Q_z^U$, and $M_y^U$ at x=0 are determined by solving the equilibrium equations of outside of overlap region of upper adherend (i.e., $-L1< x < 0$).

**2. 1. 4. Second Method** In this method, $u_a(x,z)$ and $w_a(x,z)$ may be assumed as appropriate estimating functions of $z$ (in the thickness direction). These functions have two unknown coefficients that must be determined by considering the continuity of displacements at the interfacial surfaces of the adherends and adhesive. With this in mind, considering a linear estimating function for variations of $u_a(x,z)$ and $w_a(x,z)$ along the $z$-direction, it may be written:

$$
u_a^L = u_\circ^L - \frac{h^L}{2}\psi_x^L, \quad w_a^L = w_\circ^L \quad ; \quad z = \frac{t_a}{2} \tag{25}
$$

$$
u_a^U = u_\circ^U + \frac{h^U}{2}\psi_x^U, \quad w_a^U = w_\circ^U \quad ; \quad z = -\frac{t_a}{2} \tag{26}
$$

Linear combination of Equations (25) and (26) through the adhesive thickness yields:

$$
\begin{aligned}
u_a(x,z) &= \frac{1}{t_a}\left( -u_\circ^U - \frac{h^U}{2}\psi_x^U + u_\circ^L - \frac{h^L}{2}\psi_x^L \right) z\\
&+ \frac{1}{2}\left( u_\circ^U + \frac{h^U}{2}\psi_x^U + u_\circ^L - \frac{h^L}{2}\psi_x^L \right)\\
w_a(x,z) &= \frac{-w_\circ^U + w_\circ^L}{t_a} z + \frac{w_\circ^U + w_\circ^L}{2}
\end{aligned}
\tag{27}
$$

Thus, substituting Equations (27) into the stress functions of adhesive layer (i.e., Equations (11)) gives the statements of peel and shear stresses in the adhesive layer as:

$$
\begin{aligned}
\sigma_{a,z} &= \frac{E}{1-\nu^2}\frac{\partial w_a}{\partial z} = \frac{E(-w_\circ^U + w_\circ^L)}{t_a(1-\nu^2)}\\
\tau_{a,xz} &= G\left( \frac{\partial u_a}{\partial z} + \frac{\partial w_a}{\partial x} \right)\\
&= G\left[ \frac{1}{t_a}\left( -u_\circ^U - \frac{h^U}{2}\psi_x^U + u_\circ^L - \frac{h^L}{2}\psi_x^L \right) \right.\\
&\left. + \left( -\frac{z}{t_a} + \frac{1}{2} \right)\frac{\partial w_\circ^U}{\partial x} + \left( \frac{z}{t_a} + \frac{1}{2} \right)\frac{\partial w_\circ^L}{\partial x} \right]
\end{aligned}
\tag{28}
$$

As it can be seen, the peel and shear stresses, $\sigma_{a,z}$ and $\tau_{a,xz}$, are also functions of the identified parameters which are specified for the adherends. Therefore, the governing equations may be obtained in the form of $\{dX/dx\} = [A]\{X\}$ which is a system of 12 fully coupled differential equations (see Appendix). According to what was previously discussed about the boundary conditions, an analytical solution in the form of $\{X(x,z)\} = \{X_{x=0}\} e^{[A]x}$ exists for this system.

**2. 2. Modeling the Outside of the Overlap** As Figure 1 illustrates, the outside of the overlap region includes only one of the adherends. Therefore, the equations of displacement and slope for the adherend may be written like those of the inside of the overlap zone (i.e., Equation (5)).Furthermore, the equilibrium equations are the same, the only difference is that the effects of external forces of the adhesive layer at the boundary regions are eliminated. Thus, the variation of the strain energy of the adherend may be written like

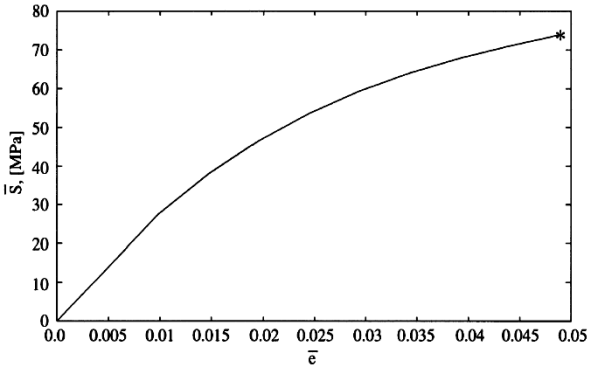


**Figure 3.** Stress-strain diagram for Epoxy AY103 (Ciba Geigy).

Equation (7). That is,

$$\delta U = \int_0^L \iint_A \left(\sigma_{xx}\delta\varepsilon_{xx} + \tau_{xz}\delta\varepsilon_{xz}\right) dA dx$$
$$= \int_0^L \left\{ -\frac{dN_x}{dx}\delta u_\circ - \frac{dM_y}{dx}\delta\psi_x + Q_z\delta\psi_x \right. \tag{29}$$
$$\left. -\frac{dQ_z}{dx}\delta w \right\} dx + \left[ N_x\delta u_\circ + M_y\delta\psi_x + Q_z\delta w \right]_0^L = 0$$

The virtual work done by external forces on the upper and lower adherends is zero (i.e., $\delta V$=0). Therefore, the equilibrium equations can be written as follows:

$$\delta u_\circ : \ \frac{dN_x}{dx} = 0, \quad \delta\psi_x : \ \frac{dM_y}{dx} = Q_z, \quad \delta w : \ \frac{dQ_z}{dx} = 0 \tag{30}$$

Equation (30) and the equations of displacement and slope of the adherend (i.e., Equation (5)) form a system of 6 differential equations as $\{dX/dx\}=[A]\{X\}$ which has an analytical solution like $\{X(x)\}=\{X_{x=x_0}\}e^{[A]x}$.

## 3. ANALYSIS OF A COMMON ADHESIVELY BONDED COMPOSITE SLJ

At first, the mechanical behavior of a common adhesively bonded SLJ is modeled as what ASTM D1002 standard has suggested, and then the analytical solutions obtained by employing the formerly discussed second method will be presented. It should be noted that, both the adherends are made of Glass/Epoxy laminates, and the adhesive is chosen to be Epoxy AY103. Epoxies have several applications in aeronautical and marine industries. Moreover, they have better mechanical properties in comparison with other types of adhesives, yet they are more expensive in cost. The stress-strain curve of Epoxy AY103, as it can be seen in Figure 3, is approximately linear.

Referred to the ASTM D1002 standard, configuration and geometrical dimensions of this SLJ are shown in Figure 4. Each adherend is made of eight unidirectional Glass/Epoxy laminates with identical thickness of $t$ = 0.2 mm (i.e. $h^L = h^U$ = 1.6 mm) and fiber stacking sequence of $(0/45/-45/90)_s$. Furthermore, the mechanical properties and thickness of adherends and adhesive layer are listed in Table 1.

**TABLE 1.** Mechanical properties and thicknesses of adhesive layer and adherends

| | Adhesive | Adherends |
|---|---|---|
| Young's modulus | $E_a$ = 2.8 GPa | $E_1$ = 36.8 GPa, $E_2 = E_3$ = 8.27 GPa |
| Shear modulus | $G_a = E_a/2(1+\nu_a)$ | $G_{12} = G_{13}$ = 4.14 GPa, $G_{23}$ = 3 GPa |
| Poisson's ratio | $\nu_a$ = 0.4 | $\nu_{12} = \nu_{13}$ = 0.26, $\nu_{23}$ = 0.38 |
| Thickness | $t_a$ = 0.33 mm | $h^L = h^U$ = 1.6mm |

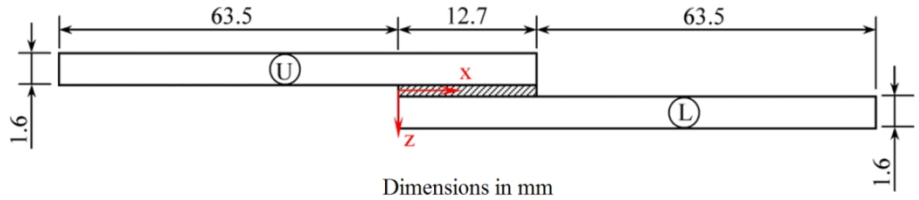


**Figure 4.** Geometrical dimensions of the SLJ corresponding to the ASTM D1002 [27].

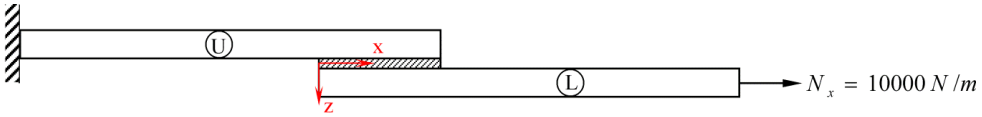


**Figure 5.** SLJ with fixed-free end conditions subjected to uniaxial tension.

## 4. RESULTS AND DISCUSSION

In order to verify the credibility of results obtained within the theory presented in this paper, an adhesively bonded SLJ with fixed-free end conditions subjected to uniaxial tensile load is studied (see Figure 5). The results are compared with those obtained using the commercial finite element software ANSYS. Figure 6 illustrates that there is a good agreement between results obtained using these two different methods, which verifies the credibility of the analytical method presented in this paper. Moreover, the results of current method including the peel stress distributions on the mid-surface of the adhesive layers of thin- and thick-adhesive single-lap joints under uniaxial loading are verified by comparing with those presented in Ref. [25]. Figure 7 illustrates a good agreement between the results for both single-lap joints. The interfacial stress distributions at the upper and lower interfaces and the mid-surface of the adhesive layer of the SLJ illustrated in Figure 5 are plotted in Figure 8. Although the shear stress distributions show some different values approaching the ends of the bonding region; the peel stress does not show significant change through the thickness. The maximum values of the shear stress distributions, as it is expected, occur near the fixed end of the SLJ. Away from the lower interface and approaching the upper one, the maximum shear stress increases about 45 percents.

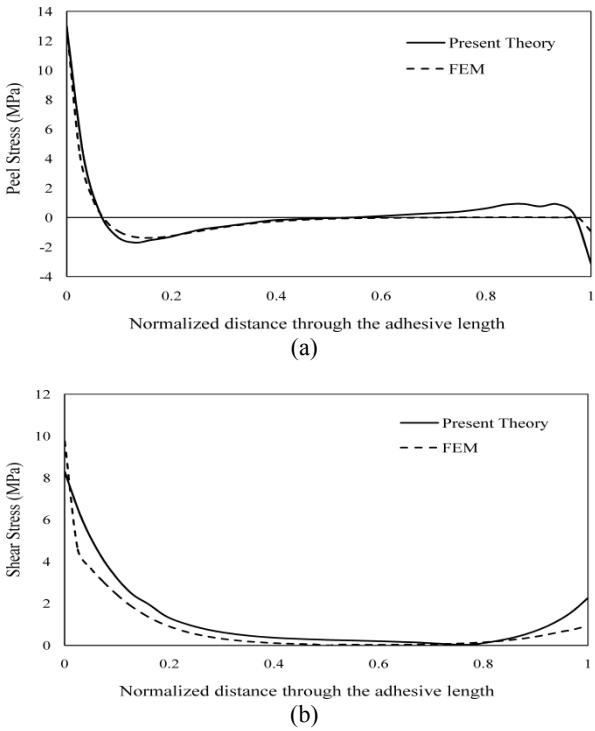


**Figure 6.** Comparison of interfacial stress distributions obtained by the present theory with those obtained by ANSYS software, (a) peel stress and (b) shear stress.

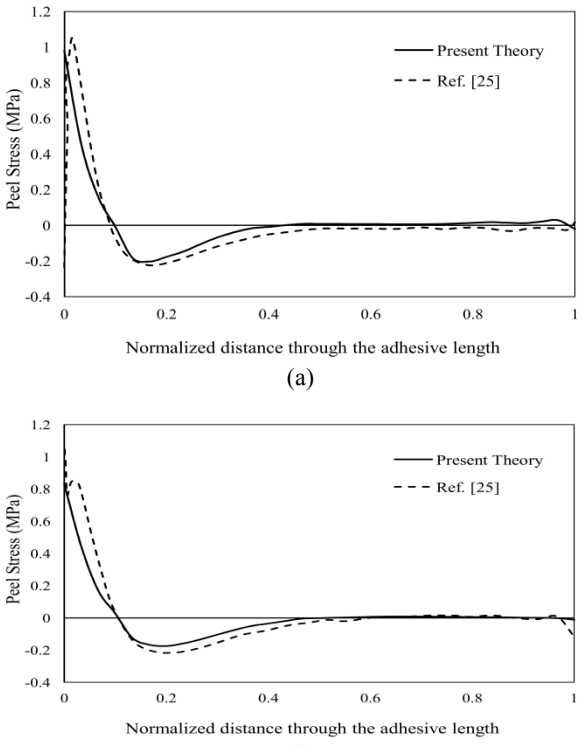


**Figure 7.** Comparison of interfacial peel stress distributions obtained by the present theory with those presented in Ref. [25], (a) thin-adhesive joint and (b) thick-adhesive joint.

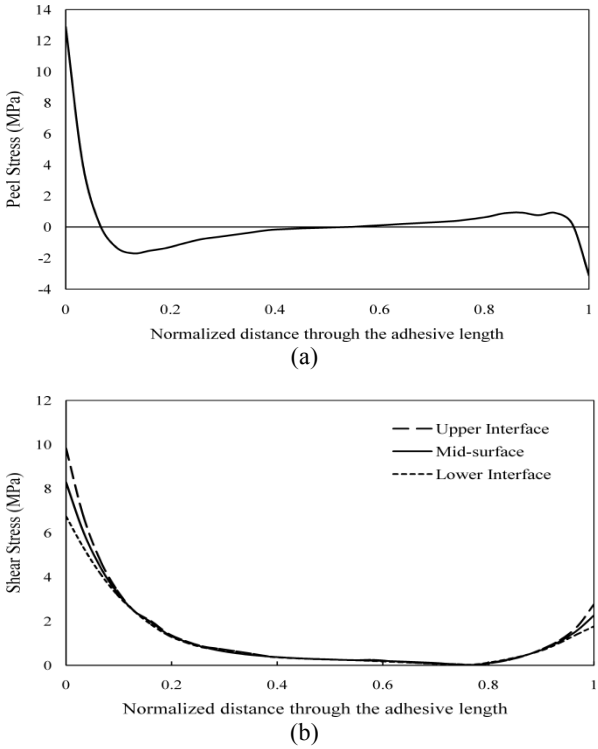


**Figure 8.** Interfacial stress distributions through the length of the bonding region of the SLJ with fixed-free end conditions under uniaxial tensile load, (a) peel stress and (b) shear stress.

This confirms the importance of using this analytical method instead of those methods which ignore the thickness effects. Another sample investigated in this paper is an adhesively bonded SLJ with pin-roll end conditions subjected to uniaxial tensile load (see Figure 9). The distributions of the peel and shear stress through the adhesive length are shown in Figure 10. It is seen that the interfacial stress components experience great variations near the edges; while, their values decreases to zero going away from the ends of the bonding region.

Comparing the results presented in Figures 8 and 10 expresses that the maximum values of the shear stresses for the SLJ with fixed-free end conditions are considerably more than those of SLJ with pin-roll end conditions. Moreover, the peel stress near the right end of the bonding region has negative values (or equivalently the compressive stress state) for fixed-free end condition; while it has positive values for pin-roll end condition. An adhesively bonded SLJ with fixed-free end conditions subjected to bending moment is investigated as the final sample. The boundary and loading conditions are defined as illustrated in Figure 11. The peel and shear stress distributions through the length of the bonding region are plotted in Figure 12.

This figure indicates that imposing a small bending moment on the right end of this SLJ can cause great values of stresses in the bonding region. Therefore, in designing the bonded joints, this kind of loading conditions must be prevented to occur as much as possible.

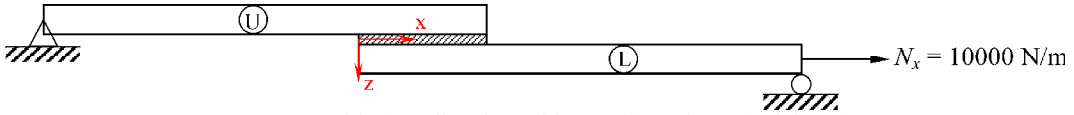


**Figure 9.** SLJ with pin-roll end conditions subjected to uniaxial tension.

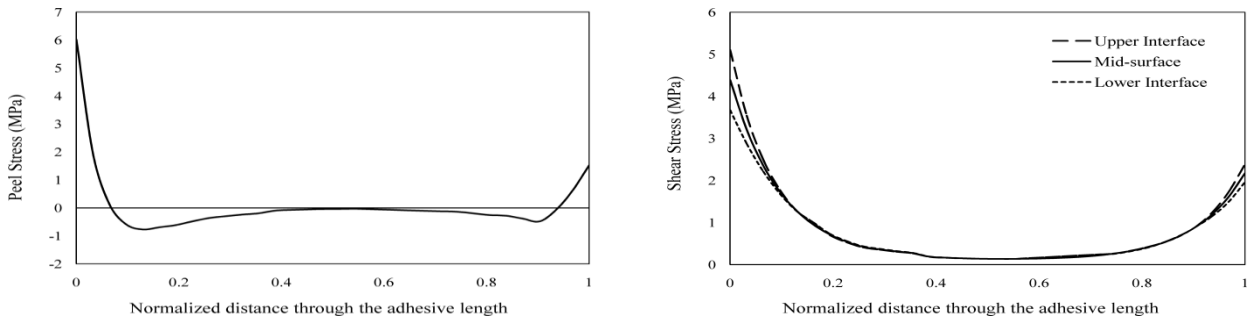


(a) (b)

**Figure 10.** Interfacial stress distributions through the length of the bonding region of the SLJ with pin-roll end conditions under uniaxial tensile load, (a) peel stress and (b) shear stress.

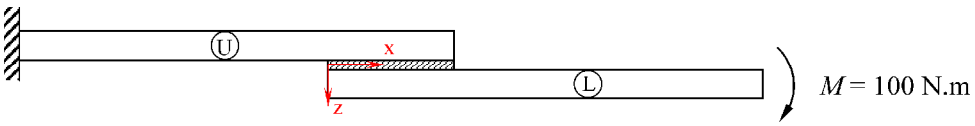


**Figure 11.** SLJ with fixed-free end conditions subjected to bending moment.

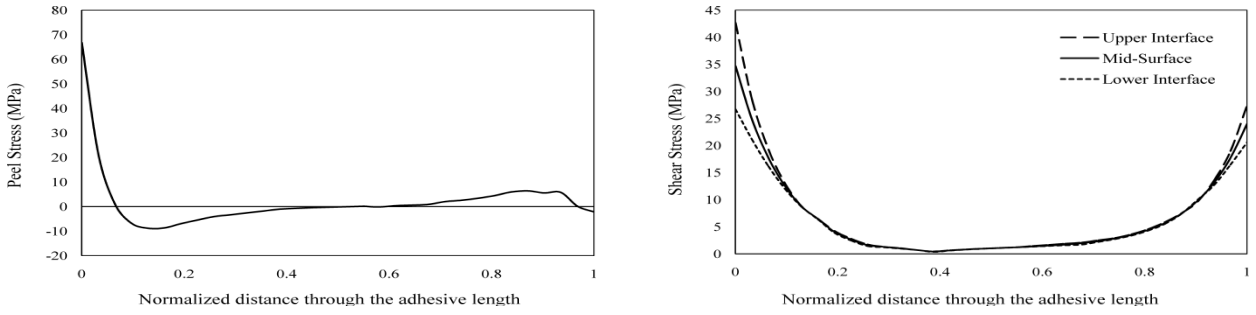


(a) (b)

**Figure 12.** Interfacial stress distributions through the length of the bonding region of the SLJ with fixed-free end conditions under bending moment, (a) peel stress and (b) shear stress.

## 5. CONCLUSIONS

This paper presents new analytical solutions to adhesively bonded composite single-lap joints with different boundary and loading conditions using the energy method and Timoshenko's beam theory. Some important conclusions drawn within this paper are stated below:

- The shear stress distribution experiences significant changes through the thickness of adhesive layer particularly near the end-points. But no considerable change of the peel stress can be seen through the adhesive thickness.
- Neither the peel nor the shear stress distribution is symmetric along the bonding region due to asymmetrical geometry, loading, and boundary conditions.
- Generally, the extreme values of both peel and shear stresses in the adhesive layer occur at one of end-points of the bond-line. Therefore, these points are intensively susceptible regions to failure.
- The loading and boundary conditions can significantly affect the interfacial stress distributions in adhesive layer. Thus, it is important to appropriately design the joint according to the applications in order to avoid its unforeseen and sudden failure.

## 6. REFERENCES


1. Zou, G., Shahin, K. and Taheri, F., "An analytical solution for the analysis of symmetric composite adhesively bonded joints", ***Composite Structures***, Vol. 65, No. 3, (2004), 499-510.
2. Tomblin, J. S., Yang, C. and Harter, P., Investigation of thick bondline adhesive joints., DTIC Document. (2001)
3. Zhu, Y. and Kedward, K., "Methods of analysis and failure predictions for adhesively bonded joints of uniform and variable bondline thickness", Office of Aviation Research, Federal Aviation Administration, (2005).
4. Arenas, J. M., Narbón, J. J. and Alía, C., "Optimum adhesive thickness in structural adhesives joints using statistical techniques based on weibull distribution", ***International Journal of Adhesion and Adhesives***, Vol. 30, No. 3, (2010), 160-165.
5. Volkersen, O., "Die nietkraftverteilung in zugbeanspruchten nietverbindungen mit konstanten lashenquerschnitten", ***Luftfahrt-Forschung***, Vol. 15, No., (1938), 41-47.
6. Goland, M. and Reissner, E., "The stresses in cemented joints", ***Journal of Applied Mechanics***, Vol. 11, No. 1, (1944), A17-A27.
7. Hart-Smith, L., "Adhesive-bonded double-lap joints", National Aeronautics and Space Administration, (1973).
8. Hart-Smith, L., "Adhesive-bonded scarf and stepped-lap joints", (1973).
9. Hart-Smith, L. J., "Adhesive-bonded single-lap joints", Langley Research Center Hampton, VA, (1973).
10. Adams, R. and Peppiatt, N., "Stress analysis of adhesive-bonded lap joints", ***The Journal of Strain Analysis for Engineering Design***, Vol. 9, No. 3, (1974), 185-196.
11. Bogdanovich, A. E. and Kizhakkethara, I., "Three dimensional finite element of double lap composite adhesive bonded joint using sub modeling approach", ***Composites Part B***, Vol. 30, No., (1999), 537-571.
12. Venkateswara Rao, M., Mohana Rao, K., Rama Chandra Raju, V., Bala Krishna Murthy, V. and Sridhara Raju, V., "Analysis of adhesively bonded single lap joints in laminated frp composites subjected to transverse load", ***in International Journal of Mechanics and Solids***, (2007).
13. Rao, G. N., Rao, M. V., Rao, K. M., Raju, V. R., Murthy, V. B. K., and Raju, V. V. S., "Analysis of adhesive bonded single lap joints in hybrid composites subjected to transverse load with s-send conditions", ***International Journal of Mechanics and Solids***, Vol. 4, No. 1, (2009), 85-94.
14. Kamal Krishna, R., Sajikumar, K. and Kumar, N. A., "Finite element analysis of composite bonded single lap joint under axial tensile force", (2010).
15. Selahi, E., Rajabi, I., Behzadi, M. and Kadivar, M. H., Analysis of adhesive double lap joint for composite materials, in International Conference on Recent Advances in Composite Materials.: Varanasi, India. (2004) 232-235.
16. Selahi, E., Rajabi, I., Jamali, M. J. and Kadivar, M. H., Analysis of adhesive double strap joint for composite materials, in International Conference on Recent Advances in Composite Materials.: Varanasi, India. (2004) 208-213.
17. Selahi, E., Rajabi, I. and Kadivar, M. H., Mathematical modeling of composite single scarf adhesive joint, in 13th International Mechanical Engineering Conference.: Isfahan, Iran. (2005)
18. Selahi, E. and Alahyari, S. M. R., Performance investigation of different types of adhesive t-joints under axial and transverse loading, in composite structures, in 16th Annual (International) Conference on Mechanical Engineering.: Kerman, Iran. (2008)
19. Selahi, E., Rajabi, I. and Alahyari, S. M. R., *I*nvestigation of relative bonded length and thicknesses of adherend and adhesive layers effects on maximum stresses in composite adhesive joints, in The 7th Iranian Aerospace Society Conference. Tehran, Iran. (2008)
20. Selahi, E., Rajabi, I. and Kadivar, M. H., Spew fillet effects on edge stress concentration of composite adhesive joints, in 15th Annual (International) Conference on Mechanical Engineering.: Tehran, Iran. (2007)
21. Chen, F. and Qiao, P., "On the intralaminar and interlaminar stress analysis of adhesive joints in plated beams", ***International Journal of Adhesion and Adhesives***, Vol. 36, (2012), 44-55.
22. Diaz Diaz, A., Hadj-Ahmed, R., Foret, G. and Ehrlacher, A., "Stress analysis in a classical double lap, adhesively bonded joint with a layerwise model", ***International Journal of Adhesion and Adhesives***, Vol. 29, No. 1, (2009), 67-76.
23. Yousefsani, S. A. and Tahani, M., "Accurate determination of stress distributions in adhesively bonded homogeneous and heterogeneous double-lap joints", ***European Journal of Mechanics-A/Solids***, (2012).
24. Abdolmajid Yousefsani, S. and Tahani, M., "Analytical solutions for adhesively bonded composite single-lap joints under mechanical loadings using full layerwise theory", ***International Journal of Adhesion and Adhesives***, (2013).
25. da Silva, L. F., das Neves, P. J., Adams, R. and Spelt, J., "Analytical models of adhesively bonded joints—part i: Literature survey", ***International Journal of Adhesion and Adhesives***, Vol. 29, No. 3, (2009), 319-330.
26. da Silva, L. F., das Neves, P. J., Adams, R., Wang, A. and Spelt, J., "Analytical models of adhesively bonded joints—part ii: Comparative study", ***International Journal of Adhesion and Adhesives***, Vol. 29, No. 3, (2009), 331-341.
27. Adams, R. D., "Structural adhesive joints in engineering", Springer, (1997).

## APPENDIX

System of 12 fully coupled differential equations:

$$\frac{du_0^U}{dx} = \frac{D_{11}^U N_x^U - B_{11}^U M_y^U}{A_{11}^U D_{11}^U - B^{U\,2}_{11}}$$

$$\frac{d\psi_x^U}{dx} = \frac{B_{11}^U N_x^U - A_{11}^U M_y^U}{B^{U\,2}_{11} - A_{11}^U D_{11}^U}$$

$$\frac{dw^U}{dx} = \frac{Q_z^U}{k_s A_{55}^U} - \psi_x^U$$

$$\frac{dQ_z^U}{dx} = \frac{E\left(w_\circ^U - w_\circ^L\right)}{t_a\left(1-\upsilon^2\right)}$$

$$\frac{dN_x^U}{dx} = G\left[\frac{1}{t_a}\left(u_\circ^U + \frac{h^U}{2}\psi_x^U - u_\circ^L + \frac{h^L}{2}\psi_x^L\right) - \frac{1}{k_s A_{55}^U}Q_z^U + \psi_x^U\right]$$

$$\frac{dM_y^U}{dx} = Q_z^U + \frac{h^U}{2}G\left[\frac{1}{t_a}\left(u_\circ^U + \frac{h^U}{2}\psi_x^U - u_\circ^L + \frac{h^L}{2}\psi_x^L\right) - \frac{1}{k_s A_{55}^U}Q_z^U + \psi_x^U\right]$$

$$\frac{du_0^L}{dx} = \frac{D_{11}^L N_x^L - B_{11}^L M_y^L}{A_{11}^L D_{11}^L - B^{L\,2}_{11}}$$

$$\frac{dN_x^L}{dx} = G\left[\frac{1}{t_a}\left(-u_\circ^U - \frac{h^U}{2}\psi_x^U + u_\circ^L - \frac{h^L}{2}\psi_x^L\right) + \frac{1}{k_s A_{55}^L}Q_z^L - \psi_x^L\right]$$

$$\frac{dM_y^L}{dx} = Q_z^L + \frac{h^L}{2}G\left[\frac{1}{t_a}\left(u_\circ^U + \frac{h^U}{2}\psi_x^U - u_\circ^L + \frac{h^L}{2}\psi_x^L\right) - \frac{1}{k_s A_{55}^L}Q_z^L + \psi_x^L\right]$$

$$\frac{d\psi_x^L}{dx} = \frac{B_{11}^L N_x^L - A_{11}^L M_y^L}{B^{L2}_{11} - A_{11}^L D_{11}^L}$$

$$\frac{dw^L}{dx} = \frac{Q_z^L}{k_s A_{55}^L} - \psi_x^L$$

$$\frac{dQ_z^L}{dx} = \frac{E\left(-w_\circ^U + w_\circ^L\right)}{t_a\left(1-\nu^2\right)}$$

# Analytical Solutions of Stress Field in Adhesively Bonded Composite Single-lap Joints under Mechanical Loadings

E. Selahi, M. Tahani, S. A. Yousefsani

*Department of Mechanical Engineering, Faculty of Engineering, Ferdowsi University of Mashhad, Mashhad, Iran*

*P A P E R I N F O*

*Paper history:*
Received 27 February 2013
Received in revised form 29 June 2013
Accepted 22 August 2013

*Keywords*:
Adhesive Bonding
Composite Joint
Interlaminar Stress
Analytical Solution

**چکیده**

در این مقاله، روشی جدید برای پیش بینی توزیع تنش های میان لایه ای عمودی و برشی در لایه چسب اتصالات چسبی کامپوزیتی تک-لبه معرفی گردیده و نتایج تحلیل برای یک نمونه استاندارد ASTM ارائه می شود. در این روش، معادلات تعادل با استفاده از روش انرژی و بر اساس تئوری تیر تیموشنکو استخراج می گردد. در ادامه دو روش حل معرفی می شود که یکی از آن ها پاسخ را بر اساس روش حساب تغییرات مستقیم و تقریب Ritz به دست می دهد؛ درحالی‌که روش دوم بر پایه یک تابع تخمینی خطی استوار است. برخلاف روش های پیشین، که در آن ها از تغییرات تنش در راستای ضخامت چسب صرفنظر شده و یا این تغییرات به صورت خطی درنظر گرفته می شود و از این رو، قادر به تحلیل اتصالات با لایه چسب ضخیم نیستند، روش حاضر با در نظر گرفتن اثرات ضخامت لایه چسب، امکان تحلیل اتصالات با لایه چسب ضخیم و نازک را فراهم می آورد.

**doi:** *10.5829/idosi.ije.2014.27.03c.16*